PAPER

In silico modeling of tibial fatigue life in physically active males and females during different exercise protocols

To cite this article: Elliot Paul *et al* 2022 *Biomed. Phys. Eng. Express* **8** 035019

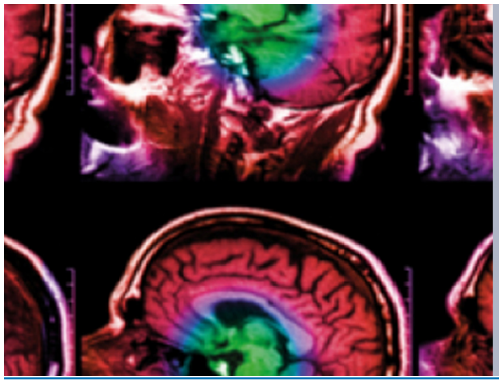

Biomedical Physics & Engineering Express

PAPER

In silico modeling of tibial fatigue life in physically active males and females during different exercise protocols

RECEIVED
12 December 2021

REVISED
25 March 2022

ACCEPTED FOR PUBLICATION
31 March 2022

PUBLISHED
8 April 2022

Elliot Paul[1], **Anup Pant**[1], **Stephanie George**[1], **John Willson**[2], **Stacey Meardon**[2] **and Ali Vahdati**[1,*]

[1] Department of Engineering, College of Engineering and Technology, East Carolina University, Greenville, NC, United States of America
[2] Department of Physical Therapy, College of Allied Health Sciences, East Carolina University, Greenville, NC, United States of America
[*] Author to whom any correspondence should be addressed.

E-mail: vahdatia18@ecu.edu

Keywords: bone stress injury, computer modeling, musculoskeletal modeling, gait mechanics, fatigue life, stress fracture

Abstract

Preventing bone stress injuries (BSI) requires a deep understanding of the condition's underlying causes and risk factors. Subject-specific computer modeling studies of gait mechanics, including the effect of changes in running speed, stride length, and landing patterns on tibial stress injury formation can provide essential insights into BSI prevention. This study aimed to computationally examine the effect of different exercise protocols on tibial fatigue life in male and female runners during prolonged walking and running at three different speeds. To achieve these aims, we combined subject-specific magnetic resonance imaging (MRI), gait data, finite element analysis, and a fatigue life prediction algorithm, including repair and adaptation's influence. The algorithm predicted a steep increase in the likelihood of developing a BSI within the first 40 days of activity. In five of the six subjects simulated, faster running speeds corresponded with higher tibial strains and higher probability of failure. Our simulations also showed that female subjects had a higher mean peak probability of failure in all four gait conditions than the male subjects studied. The approach used in this study could lay the groundwork for studies in larger populations and patient-specific clinical tools and decision support systems to reduce BSIs in athletes, military personnel, and other active individuals.

1. Introduction

Bone stress injuries (BSI) have a high incidence rate, are difficult to prevent, and are highly disruptive to daily activities. The prevailing understanding of BSI etiology points to multi-factorial injury mechanisms, in part due to repetitive, cyclical loading that overwhelms and interferes with the natural bone remodeling and repair processes [1–4]. Once a BSI has developed, it can progress to a stress fracture, disrupt regular physical activity, and require significant rest time for recovery, often for 2–12 weeks [1]. BSIs are very common in athletes and military personnel because of their intense training regimens. In both groups, the tibia is one of the most common sites of BSI [2, 5–9].

Preventing BSI requires a deep understanding of the underlying causes and risk factors for the condition. This is a challenge because many factors have been correlated with BSI, including age [2, 10], race [10–12], anatomy [13–18], and other health or habitual factors [2]. Additionally, research on military personnel and athletes suggest that women are more prone to BSIs than men; reports show that women have a 2–10 times higher incidence rate of stress fracture—a severe injury as a result of undiagnosed BSI—compared to men [2, 10, 14, 19–24]. In one study, Sherk *et al* [25] reported sex-related differences in tibia characteristics to be more significant than age-related effects in contributing to BSI. They hypothesized that several factors might contribute to the sex-based differences in tibial stress injury incidence, including differences in muscle mass, bone size, and bone density [25]. Others have argued that specific menstrual patterns [26], decreases in estrogen due to menopause [27], and differences in body fat percentage [28] contribute to the differences in male and female stress injury incidence. Systematic reviews of the literature [2, 29, 30] highlight the numerous other factors that need to be considered when screening for tibial BSI risk or treating individuals with tibial BSI. Investigations relevant to modifiable factors such as training habits that offer advice for health care professionals to prevent or treat tibial BSIs seem particularly

necessary. Despite the abundance of research related to tibial BSI, very few provide measures clinicians can take to prevent or treat tibial BSIs.

Subject-specific computer modeling studies of training habits, including the effect of changes in stride length, running speed, landing patterns, and other factors on tibial stress injury formation, can provide important insights into BSI prevention [31–37]. *In silico* models may be used to simulate how the bone will respond under physiological and non-physiological loading conditions by adapting its structure and repairing damage over time. To account for the probabilistic nature of BSI, several modeling studies have utilized finite element modeling to predict stress or strain in the tibia during routine activities in combination with a Weibull distribution of failure probability [31–34, 38]. *In silico* models of bone remodeling repair and adaptation have been developed and improved for over two decades and are routinely validated against experimental bone fracture data [34, 39–46]. While adaptive bone responses and failure probability across a wide range of running speeds have been examined by Edwards *et al* [47], effects of walking and smaller increments of speed changes have not been examined before. Additionally, some previous studies have been limited to either male or female participants [48–50], and others were developed using scaled generic bone geometric models, thus lacking truly patient-specific bone geometry segmented directly from clinical images [48, 51].

This preliminary study aimed to computationally examine and collect data on the effect of different exercise protocols on tibial fatigue life in male and female runners associated with prolonged participation in walking or running at three different speeds (including each subject's preferred running speed) using subject-specific MRI-based finite element models. The hypotheses were that (1) higher running speeds would correlate with higher probability of failure and (2) females would experience a higher probability of failure compared to males.

2. Methods

2.1. Subjects

This study was conducted with approval from the Institutional Review Board and with the participants' informed written consent. Participants were healthy adults who regularly ran more than 16 km week^{-1}. Three male and three female participants, extracted from an existing data set [52], were analyzed for this study. All subjects were between 19–24 years old, with an average age of 21.7 years (SD 2.1) for males and 23.3 years (SD 0.9) for females. The average height was 186.2 cm (SD 6.7) for males and 167.8 cm (SD 6.1) for females, and the average mass was 77.4 kg (SD 5.0) for males and 65.7 kg (SD 16.1) for females.

2.2. Experimental data collection

Prior to collecting gait data, all participants were provided standardized running shoes (Saucony Progrid Ride, Lexington, MA). All participants performed an 8-minute walk-to-run treadmill warm-up, and their preferred running speed was recorded. Four gait conditions were tested and analyzed in this study: walking (1.3 m s^{-1}), preferred running, slow running (defined as 90% of the participant's preferred running speed), and fast running (defined as 110% of preferred running speed). The mean running speeds for these gait conditions in m/s are 2.29 $\pm$ 0.16 for females and 2.73 $\pm$ 0.05 for males in the slow run, 2.54 $\pm$ 0.18 for females and 3.03 $\pm$ 0.06 for males in the preferred run, and 2.79 $\pm$ 0.20 for females and 3.34 $\pm$ 0.06 for males in the fast run condition respectively. Subjects were initially allowed to run at their preferred running speed, similar to the study of Edwards *et al* [53], to minimize alterations to their natural gait mechanics.

Gait speed conditions were conducted in random order, and the subjects were given 2 min to adjust to each gait speed condition before data was collected. Each test was recorded using a 10-camera motion capture system (200 Hz, Qualysis Corporation, Gothenburg, Sweden). Each participant's forces and gait condition were collected using an instrumented force treadmill (1000 Hz, Bertec, Columbus, Ohio, USA).

Next, all participants underwent magnetic resonance imaging (MRI) of their right tibia with a 1.5-T scanner (Philips Achieva, Best, NLD). Vitamin E capsules were used as skin markers for the motion capture data and MRI data to be aligned on the same coordinate system used for gait analysis. Axial scans were conducted with T1-weighted turbo spin-echo (TSE factor 3–4, 7 mm thick/2 mm gap, 220 FOV, 1 nex, TR 400–600 ms, TE 12 ms). Coronal and sagittal scans were conducted with T1-weighted turbo spin-echo (TSE factor 3–4, 4 mm thick/1 mm gap, 480 FOV, 1 nex, TR 400–600 ms, TE 15 ms).

2.3. Data processing and musculoskeletal modeling

The trajectory of markers and ground reaction forces were filtered using a fourth-order zero-lag low-pass Butterworth filter with a 15 Hz cutoff frequency. Lower extremity joint reaction forces and moments were based on rigid body modeling, estimated body segment parameters [54], and Newton-Euler inverse dynamics. A previously established musculoskeletal model was used to estimate muscle forces across the stance phase [54]. This model considered trial-specific joint angles, force-velocity, length-tension, and force-extension relationships to estimate muscle force for 44 muscle segments across 101 points of stance. Axial, anteroposterior, and mediolateral tibial forces were calculated by vector summation of the ankle joint reaction force, which was translated to the point 15% from the distal end (the reason for this is explained in the next subsection), and the previously calculated

muscle forces (medial gastrocnemius, lateral gastrocnemius, soleus, tibialis posterior, flexor digitorum longus, flexor hallucis longus, tibialis anterior, peroneus brevis, peroneus longus, peroneus tertius, extensor digitorum longus and extensor hallucis longus). The role of the fibula in mitigating internal tibia forces was considered by reducing the forces acting within the tibia to 90% of the original ankle joint contact forces calculated in musculoskeletal modeling [33, 34, 55].

2.4. Finite element modeling

The finite element mesh was prepared using the Mimics Innovation Suite^{TM} (Materialise NV, Belgium). First, the tibia samples were segmented in Mimics Research 23.0^{TM} semi-manually. All segmentations were conducted by the same researcher. The tibia's top 15% and bottom 15% were excluded from the analysis because these regions are primarily trabecular bone and were not clearly visible in the MR images. Only cortical bone was included in the analysis because the 1.5-T MRI resolution was too low to identify and segment trabecular bone accurately. Meshing was conducted in 3-Matic 15.0^{TM} using linear tetrahedral elements with a target edge length of 0.90 mm. Mesh sensitivity analysis was conducted, and finite element analysis results were found to converge at this target edge length. The average number of elements per tibia sample was 127,601 (SD 19,184).

Finite element analysis was conducted in FEBio [56] through an automated MATLAB (MathWorks Inc., MA) script, which used functions from the GIBBON package [57]. The samples were fixed at the proximal end of the tibial shaft, and loads were applied at the distal end of the shaft. The loads represented the maximum resultant force on the tibia during the stance phase. The cortical tibia was considered as an isotropic elastic material with an elastic modulus of 17.19 GPa and a Poisson's ratio of 0.3 [34]. The volume and maximum absolute value of the principal strains of elements in the tibia were calculated and used as the input for the fatigue life prediction algorithm [31, 33].

2.5. Fatigue life analysis

The volume and strain of each element exported from finite element models were used as the input to a probabilistic mathematical model to predict tibial fatigue implemented in MATLAB (MathWorks Inc., MA) [31, 33]. The approach adopted in this study is based on the previous work in [31, 34] and accounts for bone adaptation and repair to predict the probability of bone failure over a timespan based on strain magnitude and number of loading cycles. Mathematical details of the probabilistic failure model are thoroughly covered by Taylor *et al* [32], and Taylor and Kuiper [31]. In brief, the number of cycles to failure, N_{fa}, was calculated based on equation (1), from [34], and derived from [58]:

$$N_{fa} = 2.94\Delta\varepsilon_{eq}{}^{-n} \times 10^{-9} \quad (1)$$

where ε_{eq} is the equivalent strain value accounting for bone adaptation and the experimentally-derived constant $n = 6.6$ is based on the work of Carter and Caler [59]. The equivalent strain value was calculated using the value of maximum absolute principal strain in each element.

It was assumed that new bone would form on the periosteal surface of the tibia as a result of bone mechano-adaptation. Bone adaptation was calculated by measuring an inner and outer area of the cortical region of the tibial shaft, mathematically determining an equivalent inner and outer diameter, and assuming a deposition of 4 microns on each periosteal surface per day over the initial bone cross-section. As explained and reported in a previous study, accounting for adaptation has an important effect on the predicted probability of failure [32]. The number of cycles of loading per day, N_{fa}, was divided by the subject-specific loading frequency to calculate t_f, a reference time until failure. Reference time to failure was used in the following Weibull equation to predict the probability of failure accounting for adaptation:

$$P_{fa} = 1 - \exp\left[-\left(\frac{V_s}{V_{so}}\right)\left(\frac{t}{t_f}\right)^w\right] \quad (2)$$

where P_{fa} is the cumulative probability of failure accounting for adaptation, V_s is the volume of bone being studied, V_{so} is the reference volume (96 mm^3 for young bone samples [60]), t is the time duration of the simulations in days, and w is the Weibull modulus representing the degree of scattering in the data and set to 1.2 [53]. A volume-based approach has been used previously and has been shown to closely align with BSI data [31]. The probability of repair was calculated separately with a second Weibull equation:

$$P_r = 1 - \exp\left[-\left(\frac{t}{t_r}\right)^v\right] \quad (3)$$

where P_r is the probability of repair, t_r is the reference time for repair set to 26 days, v is the Weibull modulus constant set to 2 [32], and t is the time of the study in days. Calculating the probability of failure accounting for both repair and adaptation requires taking a derivative of P_{fa} with respect to time to find Q_{fa}, the probability density function. The probability of failure accounting for repair and adaptation, P_{fra}, was calculated as

$$P_{fra} = \int_0^t Q_{fra}\,dt = \int_0^t (1 - P_r) \times Q_{fa}\,dt \quad (4)$$

Subject-specific loading frequency was normalized by assuming the same running/walking distance of 4.8 km day^{-1} for all subjects and dividing that distance by subject-specific stride lengths for each gait condition.

The algorithm for generating subject-specific models of the tibia, applying subject-specific forces

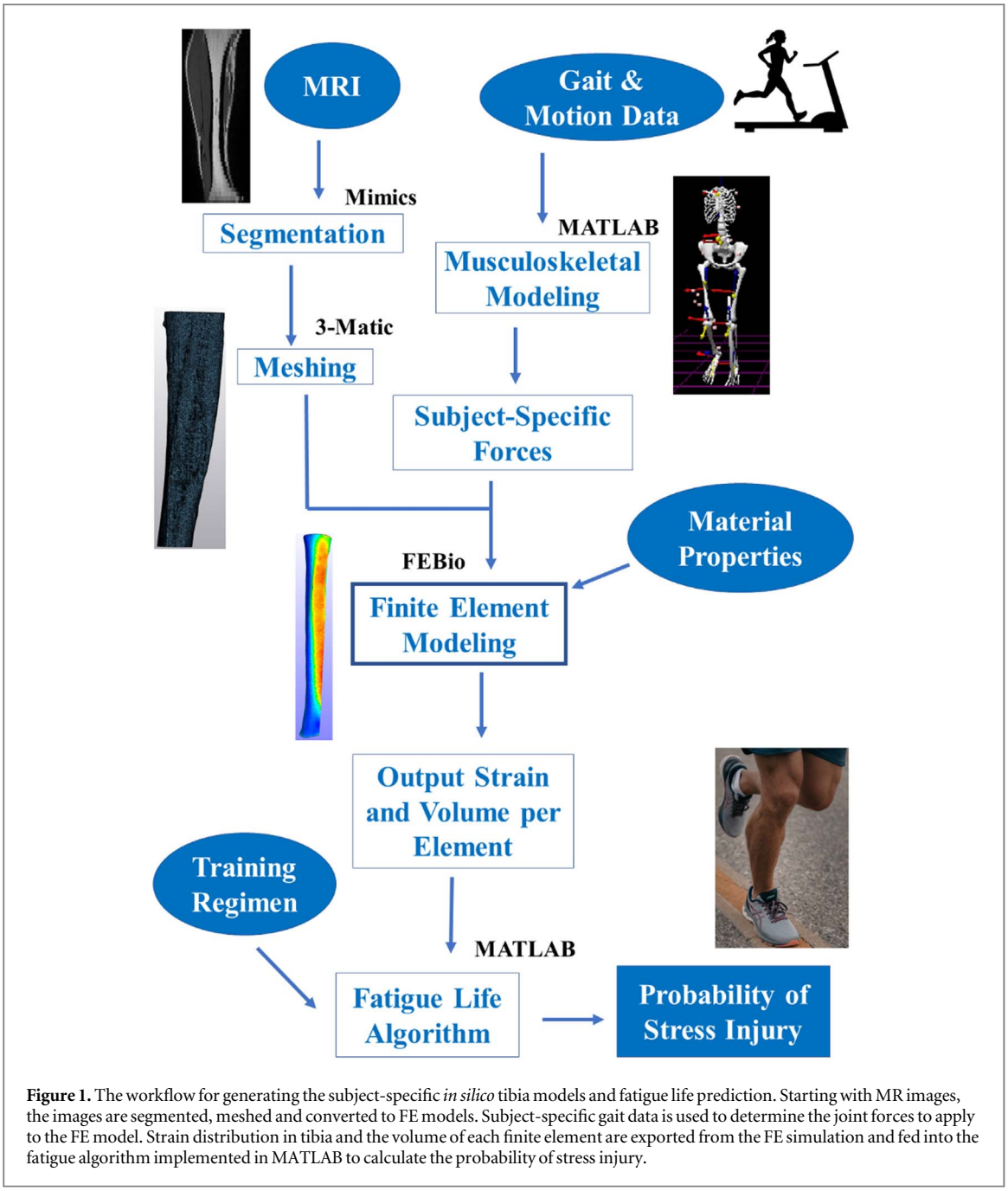

Figure 1. The workflow for generating the subject-specific *in silico* tibia models and fatigue life prediction. Starting with MR images, the images are segmented, meshed and converted to FE models. Subject-specific gait data is used to determine the joint forces to apply to the FE model. Strain distribution in tibia and the volume of each finite element are exported from the FE simulation and fed into the fatigue algorithm implemented in MATLAB to calculate the probability of stress injury.

from gait data, and estimating the probability of BSI is summarized by figure 1.

2.6. Statistical analysis

We compared the mean values between the male and females groups' outputs using one-way analysis of variance (ANOVA) in MATLAB (MathWorks Inc.), with p value smaller than 0.05 indicating statistically significant difference among means.

3. Results

While the mean walk speed for all male and female subjects was the same, ANOVA test showed the mean 'slow run', 'preferred run' and 'fast run' speeds were different between male and female subjects ($p = 0.01$ for all three cases). Table 1 shows the applied contact forces in each gait condition translated to 15% from the distal end of the tibia (where the loads were applied) as measured by gait data and musculoskeletal modeling. The most substantial component of the contact force is the axial one in all cases. On average, a 10% increase in running speed (from preferred run to fast run) produced a 4% and 9% increase in axial load in female and male subjects respectively, while a 10% decrease in running speed (from preferred run to slow run) produced an 8% and a 12% decrease in axial load in female and male subjects respectively. Anterior-posterior force and medial-lateral force made smaller contributions to the overall contact force, but were consistently higher in female subjects compared to

Table 1. Tibia forces at the centroid corresponding to the distal 15% of the tibia and mean absolute peak principal strains. Positive forces are anterior to posterior, axial compression, and medial to lateral. * Indicates statistically significant difference in mean values ($p < 0.05$) between the male (M) and female (F) subjects.

	Mean contact force (N) (mean±SD)						Mean absolute peak principal strain ($\mu\varepsilon$) (mean±SD)	
	Anterior-posterior		Axial		Medial-lateral			
Gait condition	M	F	M	F	M	F	M	F
Walk	71 ± 46	91 ± 13	4380 ± 483	3903 ± 1057	−22 ± 21	−45 ± 41	546 ± 290	745 ± 481
Slow Run	340 ± 58	390 ± 157	7906 ± 819 *	5191 ± 947 *	−10 ± 74	187 ± 79	1111 ± 731	1337 ± 911
Preferred Run	306 ± 59	401 ± 124	9000 ± 623 *	5663 ± 1092 *	−28 ± 60 *	166 ± 59 *	1232 ± 795	1413 ± 986
Fast Run	299 ± 109	427 ± 126	9790 ± 491 *	5873 ± 1032 *	−68 ± 111	209 ± 81	1406 ± 904	1562 ± 1062

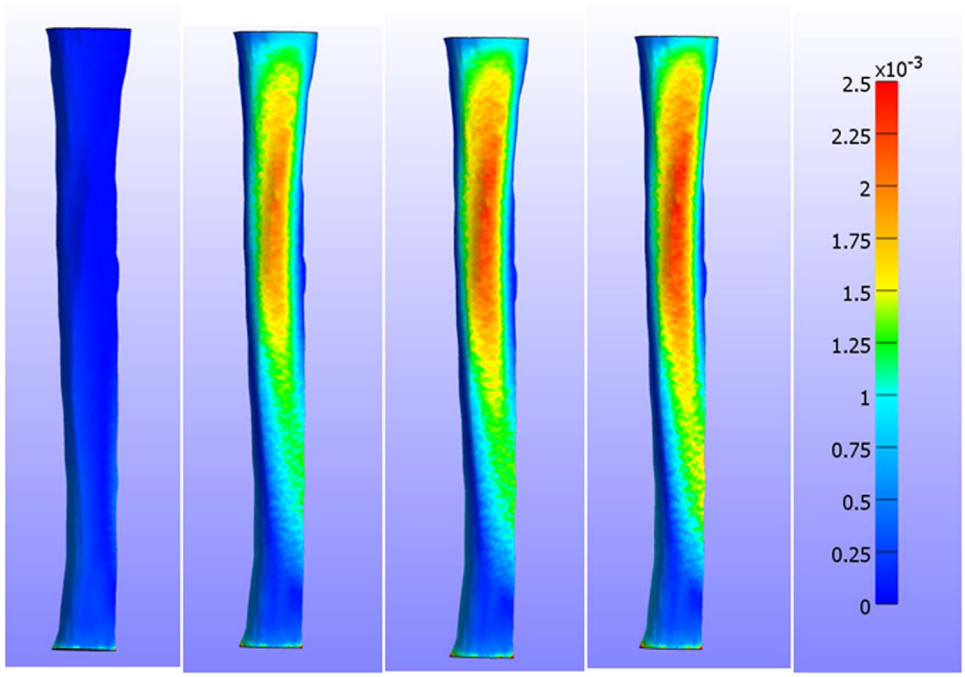

Figure 2. Posterior view of maximum principal strain distribution in subject F1 for the four different gait conditions.

males. Mean axial force showed a statistically significant difference between the male and female groups in all three running speeds.

Qualitative differences were observed in spatial distribution and magnitudes of strains predicted in the tibia by finite element analysis under the gait conditions examined. Anterior and posterior views of the maximum principal strain for one of the female subjects under all four gait conditions are displayed in figure 2. In general, the highest absolute value of principal strains was observed on the posterior surface of the tibia. Strain distribution throughout the tibia varied by gait condition. Table 1 also displays the mean absolute peak principal strains for each gait condition. In all gait conditions, female tibias experienced a higher mean absolute peak principal strain compared to males. To obtain a clearer picture of strain distribution within each tibia, the percentage of the volume of bone in each FE model for six different strain ranges are shown in figure 3 for male and female subjects separately. On average, 71% and 93% of total bone volume in the simulated tibias experienced less than 1000 $\mu\varepsilon$ in the walking condition for male and female subjects, respectively. Furthermore, a smaller volume of bone experienced less than 1000 $\mu\varepsilon$ in all three running conditions than walking. Figure 3 shows faster running conditions resulted in larger volumes of bone experiencing strains higher than 1000 $\mu\varepsilon$. For example, in female subjects, slow, preferred and fast running resulted in 43%, 41%, and 36% of bone total volume to experience strains of less than 1000 $\mu\varepsilon$, while in male subjects, slow, preferred and fast running resulted in 48%, 43% and 39% of bone total volume to experience the same low strains of less than 1000 $\mu\varepsilon$. This shows a slightly higher volume of bone in male subjects was exposed to the lowest strain range of 0–1000 $\mu\varepsilon$ versus female subjects. The difference between male and female subjects was more pronounced at higher strain ranges. For example, for the strain range of 3000–4000 $\mu\varepsilon$, in female subjects, slow, preferred and fast running resulted in 6%, 7%, and 8% of bone total volume to experience that strain range on average, while in male subjects, slow, preferred and fast running resulted in 0.4%, 2% and 5% of bone total volume to experience the same strain range on average (figure 3). We found statistically significant differences between male and female subjects in volume of bone experiencing 3000–4000 $\mu\varepsilon$ in 'slow run' and 'preferred run' case (figure 3).

Figure 4 shows a representative time history plot of BSI probability during a 100 days activity period for all four gait conditions for a female subject. The algorithm predicts a steep increase in the likelihood of developing a BSI within the first 40 days of activity. After the first 40 days, the probability of failure levels off. The peak probability of failure per subject and on average are depicted in table 2 and figure 5. Overall, the peak probability of failure was generally much lower in the walking condition compared to all three running conditions. In five of the six subjects simulated, faster running speeds were associated with higher probability of failure. For subject F2, the preferred running condition generated a smaller BSI probability than both slow and fast running gait conditions. Female subjects also displayed a higher mean peak probability of failure (the probability of failure on day 100) in all 4 gait conditions than the male subjects studied. The results for the 'slow run' case showed a

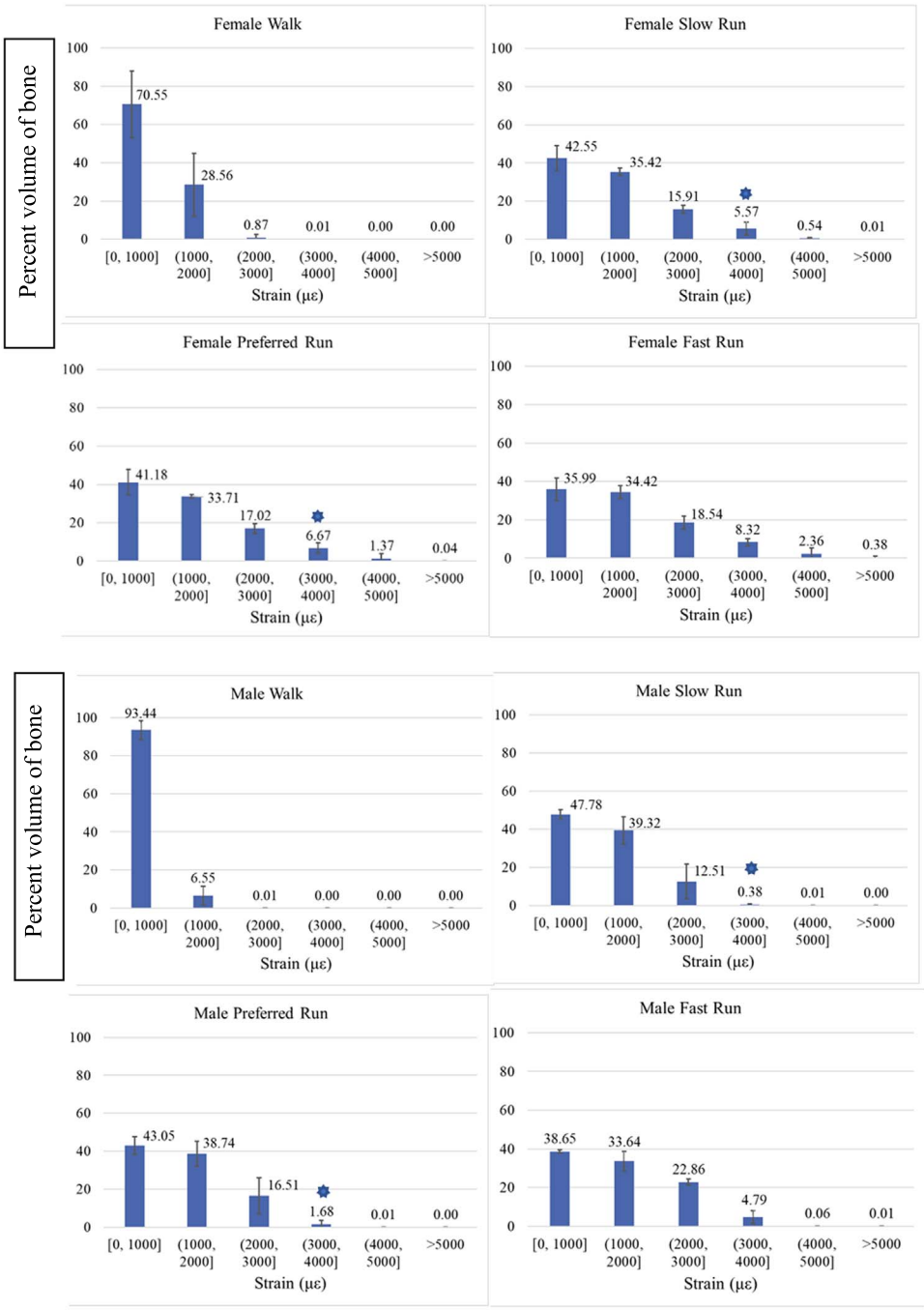

Figure 3. Distribution of maximum absolute principal strain by percentage of total bone volume experiencing each strain range between 0 to 5000 $\mu\varepsilon$ in the FE model for all four gait conditions. The results are plotted for male and female subjects separately. p value of smaller than 0.05 is shown by the symbol and indicates statistically significant difference in mean values for the male and female subjects based on ANOVA.

statistically significant difference in means between the male and female subjects (table 2).

4. Discussion and conclusion

Computational modeling and simulation provide a valuable tool to study strain distribution and damage formation in human bones non-invasively. In this study, we sought to computationally examine tibial fatigue life in physically active males and females over 100 days in walking or running at three different speeds using subject-specific loading and MRI-based bone geometry. To our knowledge, this is the first patient specific *in silico* study of male versus female tibial fatigue life that records walking and small increments between running speed.

As expected, we observed that the probability of BSI formation was generally lower for slower gait conditions (figure 5). However, moderately faster running conditions were accompanied with longer stride lengths for five of the six participants in this study.

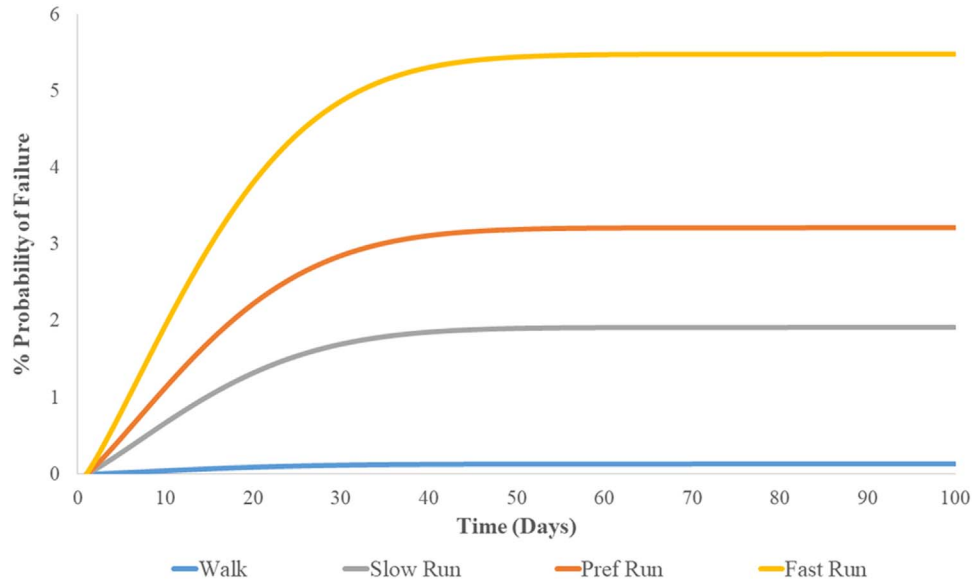

Figure 4. Probability of failure for one subject (F1) with four gait conditions assuming a distance 4.8 km day^{-1}.

Table 2. Peak probability of failure (%) for each subject and gait condition assuming 4.8 km day^{-1} for 100 days. The data in this table corresponds with the date plotted in figure 5. The table is added to make numerical comparison of failure probabilities easier for the reader and also to show the average values for each condition. p value of smaller than 0.05 indicates statistically significant difference in mean values for the male and female subjects based on ANOVA. Only the results for the 'slow run' case showed a statistically significant difference in means between the male and female subjects.

	Conditions			
Subjects	Walk	Slow run	Preferred run	Fast run
F1	0.13	1.91	3.22	5.48
F2	0.01	4.80	3.98	8.57
F3	0.07	4.44	11.8	20.36
Mean	0.07	3.72	6.33	11.47
M1	0.00	1.02	1.73	2.18
M2	0.00	0.49	0.90	3.15
M3	0.00	0.08	0.15	0.70
Mean	0.00	0.53	0.93	2.01
p value	*0.19*	*0.03*	*0.12*	*0.11*

Edwards *et al* [33, 53] studied the effects of running speed and stride length and found that reductions in running speed and stride length were associated with lower risk of stress fractures. Our results corroborate both studies because higher probability of failure in our simulations was accompanied by moderately faster running speeds, which were in turn accompanied with longer stride lengths. Our results also extend those reported by Edwards *et al* by including female subjects and by including walking, neither of which have been evaluated previously with these research methods. We expect that reductions in running speed and stride length were causes for the lower probability of stress fracture during slow running than preferred or fast running. It is interesting to note that subject F2, which had a slightly higher peak probability of failure during slow running (4.80%) than preferred running (3.98%) compared to preferred running, exhibited a longer stride length during slow running (1.92 meters) than during preferred running (1.87 meters). These results illustrate the need for personalized interventions when treating and preventing BSI.

For all gait conditions, the mean peak probability of failure for female subjects was markedly higher than for male subjects in our study, although the difference was statistically significant in the slow run scenario. These results align with BSI reports, which consistently show that women tend to have a higher BSI incidence rate than men [2, 29]. Based on our *in silico* results, we posit that differences in tibial shape and gait mechanics may be the important factors that caused the predicted higher incidence of BSI in females than males. The female subjects in our study had notably more slender tibias compared to the male subjects, which is consistent with previous studies [52, 61, 62]. The term 'slender' is used here in the context of mechanics and refers to a structural component whose length is much larger than its cross-section area. The average cross-sectional area of the cortical region of the female's tibias was 261 mm^2 (SD 60) and of the males was 350 mm^2 (SD 25) while the average leg length for female subjects was 89.2 cm (SD 4.8) and for male subjects, it was 95.6 cm (SD 5.1) clearly showing female tibias in our study were more slender than male tibias. Research suggests that people with more slender bones are at higher risk for stress injuries [15–17], so we argue that tibial geometry had some effect on the difference in predicted fatigue life for males and females. In addition to cross-sectional area, previous work has demonstrated important overall shape differences between male and female tibias [63].

In addition to tibial geometry, it has been reported that females display gait mechanics that may increase

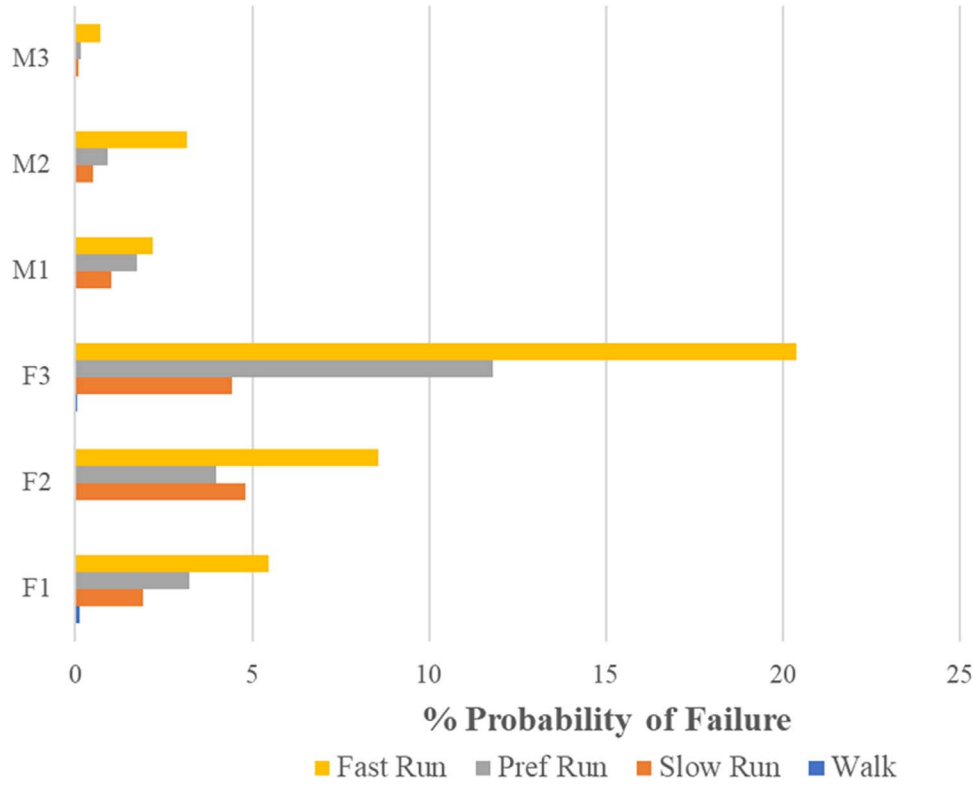

Figure 5. Peak probability of failure for each subject and the four different gait conditions assuming 4.8 km day^{-1} for 100 days.

their risk of BSI [64] as well as higher tibial stress and strain per step [52]. The nuances of gait mechanics are outside the scope of this study, but we suggest that differences in male and female gait mechanics can be a second cause for higher predicted BSI incidence in females. Interestingly, all three female subjects had a shorter stride length than all three male subjects in all gait conditions. For example, in fast running, the mean stride length for females was 28.8% shorter than for males while male subjects had a mean leg length of only 10.5% longer than the mean leg length of the female subjects. This disproportionate reduction in step length relative to limb length in females may have contributed to added load cycles necessary to travel 4.8 km, which puts the female tibias under more overall cycles of load exposure. For females, the mean number of load cycles to travel 4.8 km was 3482 (±110) for walking, 2693 (±163) for slow running, 2571 (±59) for preferred running, and 2437 (±119) for fast running. For males, the mean number of load cycles to travel 4.8 km was 3230 (±82) for walking, 2321 (±31) for slow running, 2079 (±63) for preferred running, and 1893 (±95) for fast running. In a previous computational study of systematic stride length manipulation, Edwards *et al* [53] reported that reducing the stride length by 10% can reduce the risk of BSI by 3 to 6% for a constant distance traveled despite increasing the number of load cycles. Our results do not necessarily conflict with this; rather, the females in this study displayed markedly shorter stride lengths with greater internal strain distribution per stride and a significantly greater number of load cycles that likely contributed to higher probabilities of failure. Since females subjects ran slower and had shorter strides compared to the male subjects but still showed higher tibial strains, this further supports the contention that tibial geometry is a primary determinant of BSI risk, which consequently highlights the need for subject-specific image-based FE models to predict tibial fatigue life. Muscle strength differences in males and females may also be another important determining factor explaining some of our results [52, 65].

The strains calculated from our simulations seem reasonably close to those reported in previous *in vivo* and *in silico* studies. Multiple *in vivo* studies report tensile and compressive microstrains on the tibia ranging from 1100 to 2100 $\mu\varepsilon$ during running [66, 67]. Although a portion of bone volumes in our study are estimated to have peak strains above 2100 $\mu\varepsilon$ in all three running conditions (figure 3), most of the bone volumes and the average of all tibia's peak maximum principal strains (table 1) fall in the range of experimentally measured values for all running conditions. Previous *in silico* studies often presented higher strains than what has been measured *in vivo*; Edwards *et al* [33] reported mean absolute peak principal strains between 3600 and 4600 $\mu\varepsilon$, Chen *et al* [34] reported peak strains as high as 7900 $\mu\varepsilon$. In contrast, Xu *et al* [68] reported maximum compressive strains between 860 and 3500 $\mu\varepsilon$ for women of various heights. Our reported strain values appear slightly lower than the values reported in the above studies. We believe this

may be in part due to the removal of 15% of the length of the tibia from the proximal end since the bone was not clearly visible in the MRI data. This shorter bone length may have caused an artificial increase in the rigidity of our model and therefore decreased the predicted strain values. However, this potential inaccuracy was constant across all simulations, so our results and workflow allow for a thorough qualitative comparison of the six subjects, which provides meaningful insight into BSI risk.

Our *in silico* results align with what is observed in reports on BSI incidence in the tibia, namely that intense training regimens may increase the risk of developing a BSI, which is consistent with the observation that tibia BSIs are especially common in athletes and military personnel. We believe these results indicate that *in silico* probabilistic models can be a useful tool for reducing BSI risk in the future. The goal for clinicians and trainers should be to optimize training programs so those exercise goals can be met without putting military personnel and athletes at a high risk for BSI formation. This is a delicate balance, and it may be done by including exercises that do not put high impact on the lower extremities or by having brief periods of rest at strategic time points amidst a training regimen. These potential protocol changes could be vetted with a subject-specific, computational method similar to the one we have presented. We do not claim that our results are quantitively indicative of exact BSI risks but that they qualitatively lay the groundwork for future clinical applications and additional virtual experiments in larger populations.

One limitation of this study was the relatively small sample size, which did not allow us to conduct robust statistical comparisons on male and female tibial fatigue life prediction. However, the workflow developed could be used with additional datasets to allow for robust statistical analysis. Second, this study did not control for race, lifestyle factors or physical activity history. BSIs are a multivariate condition and more extensive studies will be required to fully understand the complicated risk factors and best practices for prevention. Third, this study was based on MRI, which does not provide the same insight about subject-specific bone mechanical properties as does CT data. Unlike CT, MRI machines do not expose subjects to harmful radiation and we believe the workflow in this study provides useful insight on within-subject differences in risk of BSI and qualitative comparisons across groups. MRI is also the current gold standard for diagnosing BSI, which may increase the translatability of this work to the clinic. MRI-based workflows of bone strain may afford personalized interventions following injury in the future. That said, subject-specific training regimens based on this workflow may require CT data to calculate material properties of a subject's bone as the properties change along and within the bone. Additionally, we assumed that bone remodeling parameters are the same in all subjects. To make the models fully patient-specific, bone remodeling constants such as daily resorption and formation rates need to be defined separately for male and female subjects, and ideally for each subject in the study. Closely related, the exclusion of trabecular bone is another limitation of the study. Trabecular bone could not be included due to low-resolution images from a 1.5-T MRI scanner. However, trabecular bone has much lower elastic modulus than cortical bone; Velioglu *et al* reported trabecular bone moduli in the range of 1487–1741 MPa [69], significantly lower than the 17.19 GPa value used for cortical bone in our study. However, Tenforde *et al* classified the tibia as a cortical-rich location in the context of BSI evaluation [70]. Hence, we maintain that our results add meaningful insights despite the limitation that trabecular bone is omitted. Finally, improved modeling methods could increase the accuracy of the strains and fatigue life predicted. For example, Haider *et al* [71] suggested applying more complex boundary conditions, modeling all connected muscle forces, and modeling the fibula with a complex coupling to tibia. Similarly, Xu *et al* [68] suggested using more individualized musculoskeletal and finite element models for studying the response of female tibias to walking loads. Specifically, they pinned the tibia instead of fixing one end, applied loads to account for muscle connection sites, and used complex coupling between the tibia and fibula to account for the load-bearing properties of the fibula [68]. Accounting for the anisotropic nature of bone would be another relevant model improvement. Hoffmeister *et al* reported a range of 11.8 GPa–20.9 GPa for Young's modulus of human tibia cortical bone with the bone showing larger stiffness parallel to the long axis [72]. In the absence of CT data and patient-specific distribution of Young's modulus, adding anisotropic Young's moduli to our model would have to be based on assumed directions of anisotropy. We plan to further investigate the effect of including anisotropic mechanical properties of tibia in our analysis in future studies. We believe making these improvements to the finite element model will, in turn, improve the fatigue life predictions in future studies.

In conclusion, we provide preliminary evidence of different bone strain distribution during both walking and running in male and female subjects which has not been previously reported. We demonstrate that these methods, despite limitations, simplifications, and small sample size, are sensitive enough to demonstrate higher BSI risk in females and higher BSI risk with increased running speed. In physically active populations, the predictions of our model support the notion that prolonged and consistent exposure to modest increases in running speed are likely causes of increased BSI risk, although the small population size means most of the results were not statistically significant. Furthermore, our results showed that the largest increase in peak tibial strain magnitude and damage occurs when transitioning from a walk to run.

Our approach could be further improved and used for a larger, more comprehensive study on bone fatigue life to identify and evaluate sex-specific factors associated with tibial failure in the future. This feasibility study lays the groundwork for future patient-specific clinical tools and decision support systems to help reduce BSIs in athletes, military personnel, and other active individuals.

Acknowledgments

This material is in part based upon work supported by the National Science Foundation under Grant No. EEC-1659796 and EEC-1359183. The authors would like to thank Dr. David Taylor and Dr. Brent Edwards for their insightful email correspondence on their past work. The authors acknowledge postdoctoral salary funding (Anup Pant) and student support (Elliot Paul) from East Carolina University's Division of Research, Economic Development and Engagement.

Data availability statement

The data that support the findings of this study are available upon reasonable request from the authors.

ORCID iDs

Ali Vahdati https://orcid.org/0000-0001-7095-8407

References

[1] Jones B H, Harris J M A, Vinh T N and Rubin C 1989 Exercise-induced stress fractures and stress reactions of bone: Epidemiology, etiology, and classification *Exerc. Sport Sci. Rev.* **17** 379–422
[2] Jones B H, Thacker S B, Gilchrist J, Kimsey C D and Sosin D M 2002 Prevention of lower extremity stress fractures in athletes and soldiers: a systematic review *Epidemiologic Reviews* **24** Oxford Academic 228–47
[3] Burr D B, Martin R B, Schaffler M B and Radin E L 1985 Bone remodeling in response to *in vivo* fatigue microdamage *J. Biomech.* **18** 189–200
[4] Burr D B 1993 Remodeling and the repair of fatigue damage *Calcif. Tissue Int.* **53** S75–S81
[5] Krause G R and Thompson J R 1943 March fracture of the tibia *Radiology* **41** 580–5
[6] Leveton A L 1946 March (fatigue) fractures of the long bones of the lower extremity and pelvis *Am. J. Surg.* **71** 222–32
[7] Garcia J E, Grabhorn L L and Franklin K J 1987 Factors associated with stress fractures in military recruits *Mil. Med.* **152** 45–8
[8] Hulkko A and Orava S 1987 Stress fractures in athletes *Int. J. Sports Med.* **08** 221–6
[9] Matheson G O, Clement D B, Mckenzie D C, Taunton J E, Lloyd-Smith D R and Macintyre J G 1987 Stress fractures in athletes: a study of 320 cases *Am. J. Sports Med.* **15** 46–58
[10] Brudvig T J, Gudger T D and Obermeyer L 1983 Stress fractures in 295 trainees: a one-year study of incidence as related to age, sex, and race *Mil. Med.* **148** 666–7
[11] Friedl K E, Nuovo J A, Patience T H and Dettori J R 1992 Factors associated with stress fracture in young army women: indications for further research *Mil. Med.* **157** 334–8
[12] Gardner L I *et al* 1988 Prevention of lower extremity stress fractures: a controlled trial of a shock absorbent insole *Am. J. Public Health* **78** 1563–7
[13] Cowan D N *et al* 1996 Lower limb morphology and risk of overuse injury among male infantry trainees *Med. &amp Sci. Sport. &amp Exerc.* **28** 945–52
[14] Brunet M E, Cook S D, Brinker M R and Dickinson J A 1990 A survey of running injuries in 1505 competitive and recreational runners *J. Sports Med. Phys. Fitness* **30** 307–15 Accessed: Aug. 25, 2020. [Online]. Available: (https://europepmc.org/article/med/2266763/reload=0)
[15] Beck T J, Ruff C B, Shaffer R A, Betsinger K, Trone D W and Brodine S K 2000 Stress fracture in military recruits: gender differences in muscle and bone susceptibility factors *Bone* **27** 437–44
[16] Jepsen K J *et al* 2013 Variation in tibial functionality and fracture susceptibility among healthy, young adults arises from the acquisition of biologically distinct sets of traits *J. Bone Miner. Res.* **28** 1290–300
[17] Hadid A, Epstein Y, Shabshin N and Gefen A 2018 Biomechanical model for stress fracture-related factors in athletes and soldiers *Med. Sci. Sports Exerc.* **50** 1827–36
[18] Nunns M *et al* 2016 Four biomechanical and anthropometric measures predict tibial stress fracture: a prospective study of 1065 royal marines *Br. J. Sports Med.* **50** 1206–10
[19] Jones B H, Bovee M W, Iii M H and Cowan D N 1993 Intrinsic risk factors for exercise-related injuries among male and female army trainees *Am. J. Sports Med.* **21** 705–10
[20] Bijur P E, Horodyski M, Egerton W, Kurzon M, Lifrak S and Friedman S 1997 Comparison of injury during cadet basic training by gender *Arch. Pediatr. Adolesc. Med.* **151** 456–61
[21] Kowal D M 1980 Nature and causes of injuries in women resulting from an endurance training program *Am. J. Sports Med.* **8** 265–9
[22] Reinker K A and Ozburne S 1979 A comparison of male and female orthopaedic pathology in basic training *Mil. Med.* **144** 532–6
[23] Macleod M A, Houston A S, Sanders L and Anagnostopoulos C 1999 Incidence of trauma related stress fractures and shin splints in male and female army recruits: retrospective case study *Br. Med. J.* **318** 29
[24] Goldberg B and Pecora C 1994 'Stress fractures: a risk of increased training in freshmen *Physician and Sportsmedicine* **22** 68–78
[25] Sherk V D, Bemben D A, Bemben M G and Anderson M A 2012 Age and sex differences in tibia morphology in healthy adult caucasians *Bone* **50** 1324–31
[26] Lloyd T *et al* 1986 Women athletes with menstrual irregularity have increased musculoskeletal injuries *Med. Sci. Sport. Exerc.* **18** 374–9 Accessed: Aug. 26, 2020. [Online]. Available: (https://scholar-google-com.eu1.proxy.openathens.net/scholar?hl=en&as_sdt=0%2C5&q=Women+athletes+with+menstrual+irregularity+have+increased+musculoskeletal+injuries&btnG=)
[27] Seifert-Klauss V *et al* 2006 Influence of pattern of menopausal transition on the amount of trabecular bone loss. Results from a 6-year prospective longitudinal study *Maturitas* **55** 317–24
[28] Reid I R 2002 Relationships among body mass, its components, and bone *Bone* **31** 547–55
[29] Wentz L, Liu P Y, Haymes E and Ilich J Z 2011 Females have a greater incidence of stress fractures than males in both military and athletic populations: a systemic review *Mil. Med.* **176** 420–30
[30] Wright A A, Taylor J B, Ford K R, Siska L and Smoliga J M 2015 Risk factors associated with lower extremity stress fractures in runners: a systematic review with meta-analysis *Br. J. Sports Med.* **49** 1517–23
[31] Taylor D and Kuiper J-H The prediction of stress fractures using a 'stressed volume' concept *J. Orthop. Res.* **19** 919–26
[32] Taylor D, Casolari E and Bignardi C 2004 Predicting stress fractures using a probabilistic model of damage, repair and adaptation *J. Orthop. Res.* **22** 487–94

[33] Edwards B W, Taylor D, Rudolphi T J, Gillette J C and Derrick T R 2010 Effects of running speed on a probabilistic stress fracture model *Clin. Biomech.* **25** 372–7
[34] Chen T L, An W W, Chan Z Y S, Au I P H, Zhang Z H and Cheung R T H 2016 Immediate effects of modified landing pattern on a probabilistic tibial stress fracture model in runners *Clincal Biomechanics* **33** 49–54
[35] Garijo N, Verdonschot N, Engelborghs K, García-Aznar J M and Pérez M A 2017 Subject-specific musculoskeletal loading of the tibia: computational load estimation *Journal of The Mechanichal Behavior of Biomedical Materials* **65** 334–43
[36] Fang J, Gong H, Kong L and Zhu D 2013 Simulation on the internal structure of three-dimensional proximal tibia under different mechanical environments *Biomed. Eng. Online* **12**
[37] Cheong V S, Campos Marin A, Lacroix D and Dall'Ara E 2020 A novel algorithm to predict bone changes in the mouse tibia properties under physiological conditions *Biomech. Model. Mechanobiol.* **19** 985–1001
[38] Weibull W 1951 A statistical distribution function of wide applicability *J. Appl. Mech.* **18** 293–7
[39] Edwards W B 2018 Modeling overuse injuries in sport as a mechanical fatigue phenomenon *Exerc. Sport Sci. Rev.* **46** 224–31
[40] Taylor D 1998 Fatigue of bone and bones: An analysis based on stressed volume *J. Orthopaedic Research* **16** 163–9
[41] Pant A, Paul E, Niebur G L and Vahdati A 2021 Integration of mechanics and biology in computer simulation of bone remodeling *Prog. Biophys. Mol. Biol.*
[42] Vahdati A and Rouhi G 2009 A model for mechanical adaptation of trabecular bone incorporating cellular accommodation and effects of microdamage and disuse *Mech. Res. Commun.* **36** 284–93
[43] Vahdati A, Walscharts S, Jonkers I, Garcia-Aznar J M, Vander Sloten J and van Lenthe G H 2014 Role of subject-specific musculoskeletal loading on the prediction of bone density distribution in the proximal femur *J. Mech. Behav. Biomed. Mater.* **30** 244–52
[44] Vahdati A, Rouhi G, Ghalichi F and Tahani M 2018 Mechanically induced trabecular bone remodeling including cellular accommodation effect: A computer simulation *Transactions of the Canadian Society for Mechanical Engineering* **32** 371–81
[45] Larcher I and Scheiner S 2021 Parameter reduction, sensitivity studies, and correlation analyses applied to a mechanobiologically regulated bone cell population model of the bone metabolism *Comput. Biol. Med.* **136** 104717
[46] Peyroteo M M A, Belinha J and Natal Jorge R M 2021 A mathematical biomechanical model for bone remodeling integrated with a radial point interpolating meshless method *Comput. Biol. Med.* **129** 104170
[47] Brent Edwards W, Taylor D, Rudolphi T J, Gillette J C and Derrick T R 2010 Effects of running speed on a probabilistic stress fracture model
[48] Edwards W B, Taylor D, Rudolphi T J, Gillette J C and Derrick T R 2009 Effects of stride length and running mileage on a probabilistic stress fracture model *Med. Sci. Sport. Exerc.* **41** 2177–84
[49] Brent Edwards W, Taylor D, Rudolphi T J, Gillette J C and Derrick T R 2010 Effects of running speed on a probabilistic stress fracture model *Clin. Biomech.* **25** 372–7
[50] Unnikrishnan G *et al* 2021 Effects of body size and load carriage on lower-extremity biomechanical responses in healthy women *BMC Musculoskelet. Disord.* **22** 219
[51] Chen T L, An W W, Chan Z Y S, Au I P H, Zhang Z H and Cheung R T H 2016 Immediate effects of modified landing pattern on a probabilistic tibial stress fracture model in runners *Clin. Biomech.* **33** 49–54
[52] Meardon S A *et al* 2021 Peak and per-step tibial bone stress during walking and running in female and male recreational runners **49** 2227–37
[53] Edwards W B, Taylor D, Rudolphi T J, Gillette J C and Derrick T R 2009 Effects of stride length and running mileage on a probabilistic stress fracture model *Med. Sci. Sports Exerc.* **41** 2177–84
[54] Derrick T R, Edwards W B, Fellin R E and Seay J F 2016 An integrative modeling approach for the efficient estimation of cross sectional tibial stresses during locomotion *J. Biomech.* **49** 429–35
[55] Sasimontonkul S, Bay B K and Pavol M J 2007 Bone contact forces on the distal tibia during the stance phase of running *J. Biomech.* **40** 3503–9
[56] Maas S A, Ellis B J, Ateshian G A and Weiss J A 2012 FEBio: Finite elements for biomechanics *J. Biomech. Eng.* **134** 011005
[57] Moerman K M 2018 GIBBON: the geometry and image-based bioengineering add-On *J. Open Source Softw.* **3** 506
[58] Carter D R, Caler W E, Spengler D M and Frankel V H 1981 Fatigue behavior of adult cortical bone: the influence of mean strain and strain range *Acta Orthop. Scand.* **52** 481–90
[59] Carter D R and Caler W E 1983 Cycle-dependant and time-dependant bone fracture with repeated loading *J. Biomech. Eng.* **105** 166–70
[60] Zioupos P, Wang X T and Currey J D 1996 The accumulation of fatigue microdamage in human cortical bone of two different ages *in vitro Clin. Biomech.* **11** 365–75
[61] Franklyn M, Oakes B, Field B, Wells P and Morgan D 2008 Section modulus is the optimum geometric predictor for stress fractures and medial tibial stress syndrome in both male and female athletes *Am. J. Sports Med.* **36** 1179–89
[62] Riggs B L *et al* 2004 Population-based study of age and sex differences in bone volumetric density, size, geometry, and structure at different skeletal sites *J. Bone Miner. Res.* **19** 1945–54
[63] Tümer N *et al* 2019 Three-dimensional analysis of shape variations and symmetry of the fibula, tibia, calcaneus and talus *J. Anat.* **234** 132–44
[64] Milner C E, Ferber R, Pollard C D, Hamill J and Davis I S 2006 Biomechanical factors associated with tibial stress fracture in female runners *Med. Sci. Sports Exerc.* **38** 323–8
[65] KL P *et al* 2009 Bone geometry, strength, and muscle size in runners with a history of stress fracture *Med. Sci. Sports Exerc.* **41** 2145–50
[66] Milgrom C *et al* 2000 Do high impact exercises produce higher tibial strains than running? *Br. J. Sports Med.* **34** 195–9
[67] Ekenman I, Halvorsen K, Westblad P, Fellander-Tsai L and Rolf C 1998 Local bone deformation at two predominant sites for stress fractures of the tibia: an *in vivo* study *Foot Ankle Int.* **19** 479–84
[68] Xu C, Reifman J, Baggaley M, Edwards W B and Unnikrishnan G 2020 Individual differences in women during walking affect tibial response to load carriage: the importance of individualized musculoskeletal finite-element models *IEEE Trans. Biomed. Eng.* **67** 545–55
[69] Velioglu Z B, Pulat D, Demirbakan B, Ozcan B, Bayrak E and Erisken C 2018 3D-printed poly(lactic acid) scaffolds for trabecular bone repair and regeneration: scaffold and native bone characterization *Connective Tissue Research* **60** 274–82
[70] Tenforde A S, Parziale A L, Popp K L and Ackerman K E 2018 Low bone mineral density in male athletes is associated with bone stress injuries at anatomic sites with greater trabecular composition *Am. J. Sports Med.* **46** 30–6
[71] Haider I T, Baggaley M and Brent Edwards W 2020 Subject-specific finite element models of the tibia with realistic boundary conditions predict bending deformations consistent with *in vivo* measurement *J. Biomech. Eng.* **142** 021010
[72] Hoffmeister B K, Smith S R, Handley S M and Rho J Y 2000 Anisotropy of Young's modulus of human tibial cortical bone *Med. Biol. Eng. Comput.* **38** 333–8